ELSEVIER

Journal of Alloys and Compounds 339 (2002) 162–166

Journal of ALLOYS AND COMPOUNDS

www.elsevier.com/locate/jallcom

Transformation temperatures and second phases in Ti–Ni–Si ternary shape memory alloys with Si≤2 at.%

S.F. Hsieh[a], S.K. Wu[b,*], H.C. Lin[c]

[a]*Department of Mold and Die Engineering, National Kaohsiung University of Applied Science, Kaohsiung, Taiwan 807*
[b]*Department of Materials Science and Engineering, National Taiwan University, Taipei, Taiwan 106*
[c]*Department of Materials Science, Feng Chia University, Taichung, Taiwan 407*

Received 3 September 2001; accepted 13 November 2001

Abstract

Effects of Si on transformation temperatures and second phases in $Ti_{50-x}Ni_{50}Si_x$, $Ti_{50}Ni_{50-x}Si_x$ and $Ti_{51}Ni_{49-x}Si_x$ shape memory alloys (SMAs) with $x=1$, 2 at.% are investigated. Three different second-phase particles located at grain boundaries are observed. They are χ-phase particles ($Ti_5Ni_4Si_1$), λ_1-phase particles ($Ti_2Ni_3Si_1$) and Ti_2(Ni, Si) particles. In addition to the formation of second phases, a small amount of Si remained in solid solution in the matrix of Ti–Ni–Si ternary SMAs. Experimental results show that, in the matrix, the effects of Ni+Si in combination on transformation temperatures of Ti–Ni–Si ternary SMAs are similar to Ni effects on those of as-quenched TiNi binary SMAs.

Keywords: Transition metal compounds; Metallography; Thermal analysis; Phase transition

1. Introduction

Among many shape memory alloys (SMAs), TiNi alloys are the most feasible from the point of view of application in both shape memory effect (SME) and pseudoelasticity (PE). It has been confirmed that the properties of TiNi SMAs can be affected by various thermal–mechanical treatments, such as thermal cycling [1], aging [2,3] and cold rolling [4]. Furthermore, the addition of a third element to replace Ni and/or Ti has a substantial effect on phase transformation behavior of TiNi alloys. The starting temperature of martensitic transformation, Ms, of TiNi binary alloys decreases following the substitution of Ni with V, Cr, Mn, Fe or Co elements [5–7], but increases remarkably following the substitution of Ni with Au, Pd or Pt in amounts not less than 15–20 at.% [8–10]. At the same time, the martensitic transformation sequence can also be affected by the addition of a third element, such that the B2→B19′ sequence of $Ti_{50}Ni_{50}$ SMA changes to B2→R→B19′ in $Ti_{50}Ni_{47}Fe_3$ alloy [7], but to B2→B19→B19′ in $Ti_{50}Ni_{40}Cu_{10}$ alloy [11,12]. Here, B2 is the parent austenite of TiNi SMA, B19′ is the monoclinic martensite, R is the rhombohedral premartensite and B19 is the orthorhombic premartensite. It is well known that a small deviation from stoichiometry in TiNi SMAs can give rise to significant precipitation of second phases [13,14]. This in turn affects both the strength of the alloy and its shape memory effect. To our knowledge, transformation behavior and precipitated second phases in Ti–Ni–Si ternary SMAs with small amounts of Si have not been reported yet. The purpose of the present study is to investigate the effect of substituted Si on transformation temperatures of $Ti_{50-x}Ni_{50}Si_x$, $Ti_{50}Ni_{50-x}Si_x$ and $Ti_{51}Ni_{49-x}Si_x$ alloys with $x=1$–2 at.%. The precipitated second phases in these alloys are also discussed.

2. Experimental

The conventional tungsten arc melting technique was employed to prepare $Ti_{50-x}Ni_{50}Si_x$, $Ti_{50}Ni_{50-x}Si_x$ and $Ti_{51}Ni_{49-x}Si_x$ alloys with $x=1$, 2 at.%, i.e. $Ti_{49}Ni_{50}Si_1$, $Ti_{48}Ni_{50}Si_2$, $Ti_{50}Ni_{49}Si_1$, $Ti_{50}Ni_{48}Si_2$, $Ti_{51}Ni_{48}Si_1$ and $Ti_{51}Ni_{47}Si_2$ alloys. The as-melted buttons were homogenized at 950 °C for 72 h and then furnace cooled. The buttons were cut into several plates with a low speed diamond saw, sealed in evacuated quartz tubes, annealed at 900 °C for 2 h and then quenched in water with the tube

*Corresponding author. Tel.: +886-2-2363-7846; fax: +886-2-2363-4562.

E-mail address: skw@ccms.ntu.edu.tw (S.K. Wu).

0925-8388/02/$ – see front matter
PII: S0925-8388(01)01974-0

intact. DSC measurements were made with a Dupont 9990 thermal analyzer equipped with a quantitative scanning system 910 DSC cell for controlled heating and cooling runs on samples encapsulated in an aluminum pan and operated in N_2 atmosphere. The running temperature range was from −100 to 200 °C with a heating and cooling rate of 10 °C/min. A quantitative analysis of the chemical composition of alloys was performed by using a Joel JXA-8600SX electron probe microanalyzer (EPMA) equipped with a wavelength dispersive X-ray spectrometer (WDS) analysis system. The operating voltage of EPMA is 20 kV and the software for quantification is the XM-86PAC quantitative analysis program.

3. Results and discussion

Fig. 1(a)–(f) show the EPMA backscattering electron images (BEIs) of homogenized $Ti_{49}Ni_{50}Si_1$, $Ti_{48}Ni_{50}Si_2$, $Ti_{50}Ni_{49}Si_1$, $Ti_{50}Ni_{48}Si_2$, $Ti_{51}Ni_{48}Si_1$ and $Ti_{51}Ni_{47}Si_2$ alloys, respectively. There are three different contrast areas that can be observed in $Ti_{48}Ni_{50}Si_2$, $Ti_{50}Ni_{48}Si_2$ and

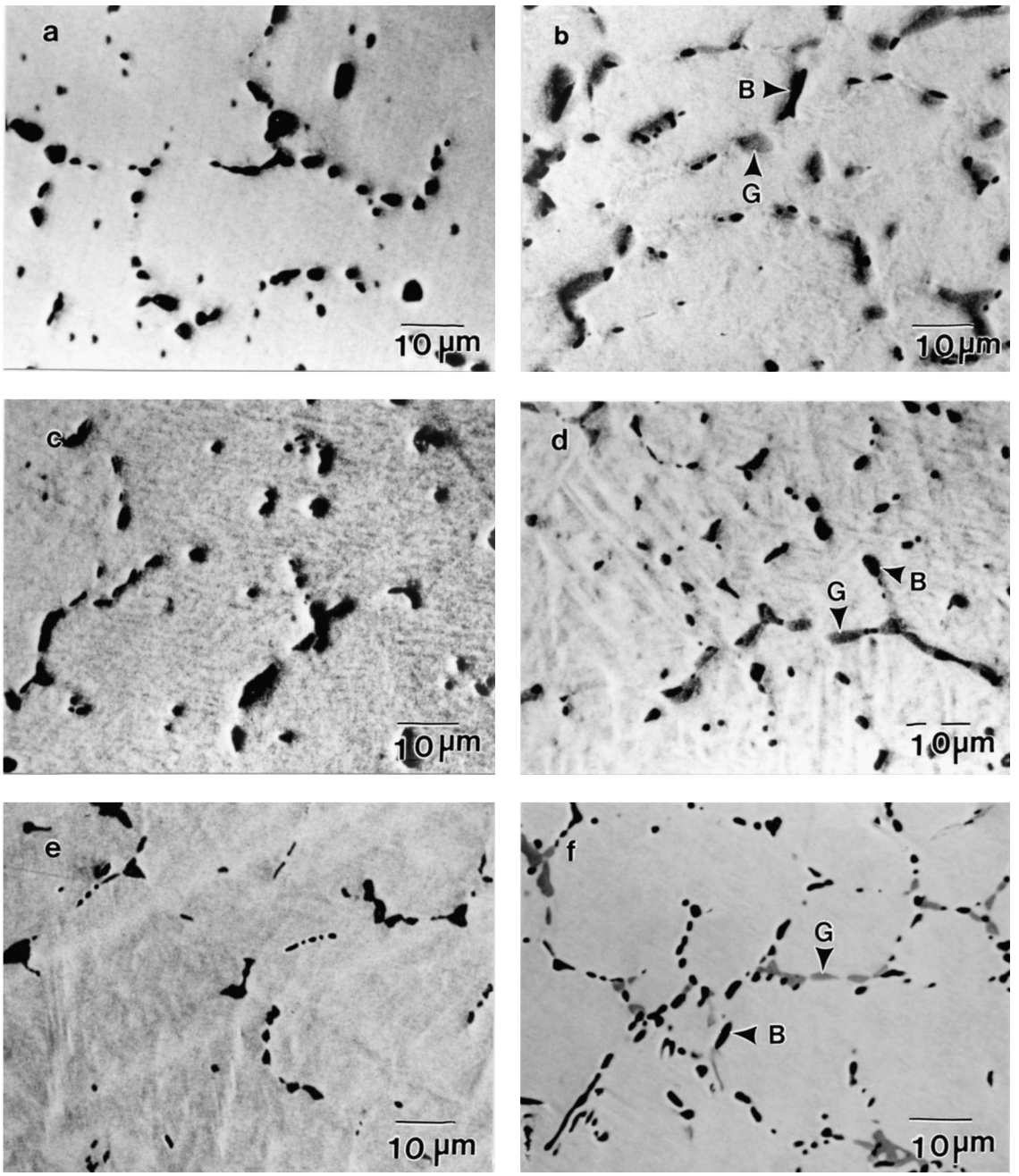

Fig. 1. EPMA backscattering electron images (BEIs) of the 950 °C homogenized (a) $Ti_{49}Ni_{50}Si_1$, (b) $Ti_{48}Ni_{50}Si_2$, (c) $Ti_{50}Ni_{49}Si_1$, (d) $Ti_{50}Ni_{48}Si_2$, (e) $Ti_{51}Ni_{48}Si_1$ and (f) $Ti_{51}Ni_{47}Si_2$ alloys. In (b), (d) and (f), B and G indicate the black and gray particles, respectively.

$Ti_{51}Ni_{47}Si_2$ alloys, including the gray matrix, the black particles and the gray particles, as shown in Fig. 1(b), (d) and (f). However, only black particles located around the grain boundaries appear in Fig. 1(a), (c) and (e) of $Ti_{49}Ni_{50}Si_1$, $Ti_{50}Ni_{49}Si_1$ and $Ti_{51}Ni_{48}Si_1$ alloys, respectively. The chemical compositions of the matrix and second-phase particles determined by WDS of EPMA are given in Table 1. The data given in Table 1 are the averages taken of at least five tests for each area with the errors. The ratios R=Ti/(Ni+Si) of the matrix and second-phase particles are also calculated in Table 1. Based on 750 and 1000 °C Ti–Ni–Si ternary phase diagrams [15], WDS chemical analysis and backscattering electron characteristics of EPMA image, Table 1 indicates that all the matrix in Fig. 1 is TiNi SMA containing a small amount of Si in solid solution. The amount of Si in solid solution in the matrix increases with the increasing amount of Si substituted in TiNiSi ternary SMAs. The black particles are the χ phase ($Ti_5Ni_4Si_1$) in $Ti_{50-x}Ni_{50}Si_x$ and $Ti_{50}Ni_{50-x}Si_x$ alloys with $x=1$, 2 at.%, but they are Ti_2(Ni, Si) phase in Ti-rich $Ti_{51}Ni_{49-x}Si_x$ alloys with $x=1$, 2 at.%. The gray particles are the λ_1 phase ($Ti_2Ni_3Si_1$) in $Ti_{48}Ni_{50}Si_2$ and $Ti_{50}Ni_{48}Si_2$ alloys, but they are χ phase in $Ti_{51}Ni_{47}Si_2$ alloy. According to Table 1, the composition of the χ phase ($Ti_5Ni_4Si_1$) appearing in Fig. 1 is in the range of 50–55 at.% Ti and 12–15 at.% Si and that of λ_1 phase ($Ti_2Ni_3Si_1$) is in the range of 33–35 at.% Ti and 16–19 at.% Si.

Fig. 2 shows the experimental results of DSC measurements for homogenized $Ti_{48}Ni_{50}Si_2$, $Ti_{50}Ni_{48}Si_2$ and $Ti_{51}Ni_{47}Si_2$ alloys. The peak temperatures M* and A* (including Ms, Mf, As and Af points) appearing in Fig. 2 are associated with the forward and reverse martensitic transformation of B2↔B19′, respectively [16]. DSC curves for $Ti_{49}Ni_{50}Si_1$, $Ti_{50}Ni_{49}Si_1$ and $Ti_{51}Ni_{48}Si_1$ alloys are similar to those of Fig. 2 and thus are omitted. All DSC results of M*, A* and Ms temperatures are listed in Table 2. From Tables 1 and 2, transformation peak temperatures, M* and A*, versus the R ratio of the matrix are plotted and shown in Fig. 3. From Fig. 3, it is clear that transformation peak temperatures increase with the increase in the R ratio up to 1.01 and then gradually levels off when the R ratio is more than 1.01. It is well known that Ms temperature increases with the increasing Ti/Ni ratio in as-quenched TiNi binary alloys [3,14]. This behavior is also shown in Fig. 3. From the results of Fig. 3 and Tables 1 and 2, it can be deduced that the Ms temperature of an equiatomic TiNi binary alloy is about 60 °C, but for $Ti_{49}Ni_{50}Si_1$ alloy and $Ti_{48}Ni_{50}Si_2$ alloys, the Ms temperature becomes approximately −24 and −47 °C, respectively, which lie between the Ms temperatures of as-quenched $Ti_{49.4}Ni_{50.6}$ alloy, Ti/Ni=0.976, −21 °C [3] and the −95 °C of as-quenched $Ti_{49}Ni_{51}$ alloy, Ti/Ni=0.961 [2]. According to Table 1, the R ratio of the matrix of $Ti_{49}Ni_{50}Si_1$ and $Ti_{48}Ni_{50}Si_2$ alloys are 0.972 and 0.967, respectively, which also fall in the range of 0.961–0.976. This fact implies that the effect

Table 1
Compositional analyses by EPMA of $Ti_{50-x}Ni_{50}Si_x$, $T_{50}Ni_{50-x}Si_x$ and $Ti_{51}Ni_{49-x}Si_x$ alloys with $x=1$, 2 at.% homogenized at 950 °C for 72 h

Alloys		Ti (at.%)	Ni (at.%)	Si (at.%)	Ti/(Si+Ni) R ratio	Remark
$Ti_{49}Ni_{50}Si_1$	M	49.29±0.15	50.54±0.16	0.17±0.06	0.972	Matrix
	B	50.35±0.26	36.27±0.30	13.38±0.21	–	χ-Phase
	G	–	–	–	–	–
$Ti_{48}Ni_{50}Si_2$	M	49.17±0.16	50.37±0.18	0.46±0.08	0.967	Matrix
	B	50.08±0.21	36.61±0.27	13.31±0.24		χ-Phase
	G	35.25±0.24	47.43±0.30	17.32±0.16	–	λ_1-Phase
$Ti_{50}Ni_{49}Si_1$	M	50.27±0.13	49.28±0.15	0.45±0.07	1.011	Matrix
	B	50.53±0.25	36.50±0.23	12.97±0.26	–	χ-Phase
	G	–	–	–	–	–
$Ti_{50}Ni_{48}Si_2$	M	50.32±0.16	48.76±0.21	0.92±0.12	1.013	Matrix
	B	50.47±0.30	35.31±0.25	14.22±0.20	–	χ-Phase
	G	35.47±0.20	47.05±0.20	17.48±0.16	–	λ_1-Phase
$Ti_{51}Ni_{48}Si_1$	M	51.06±0.20	48.72±0.18	0.22±0.06	1.043	Matrix
	B	66.39±0.27	32.14±0.25	1.47±0.18	1.980	Ti_2(Ni+Si)
	G	–	–	–	–	–
$Ti_{51}Ni_{47}Si_2$	M	51.21±0.18	47.96±0.20	0.83±0.10	1.050	Matrix
	B	67.31±0.25	31.37±0.27	1.32±0.17	2.059	Ti_2(Ni+Si)
	G	50.12±0.21	34.49±0.24	15.39±0.23	–	χ-Phase

M, matrix; B, black particles; G, gray particles; χ-Phase, $Ti_5Ni_4Si_1$; λ_1-Phase, $Ti_2Ni_3Si_1$.

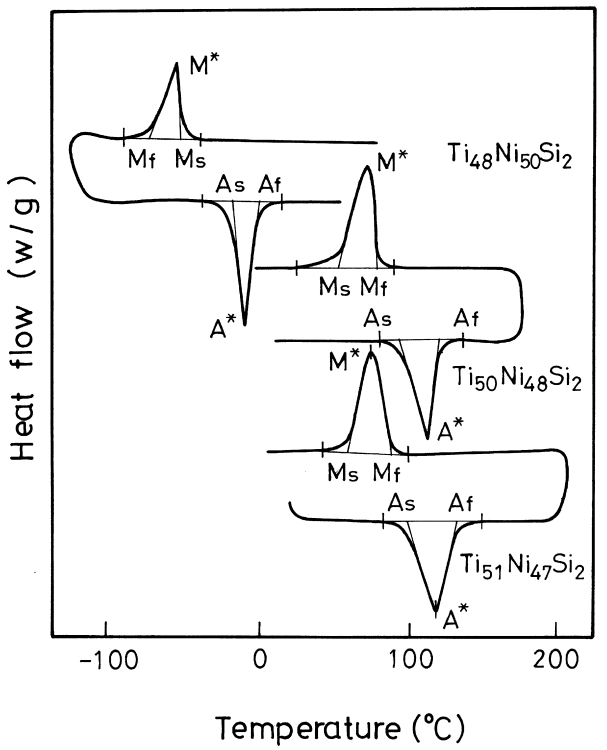

Fig. 2. DSC curves of as-annealed $Ti_{48}Ni_{50}Si_2$, $Ti_{50}Ni_{48}Si_2$ and $Ti_{51}Ni_{47}Si_2$ alloys. M* and A* are peak temperatures of forward and reverse martensitic transformation, respectively.

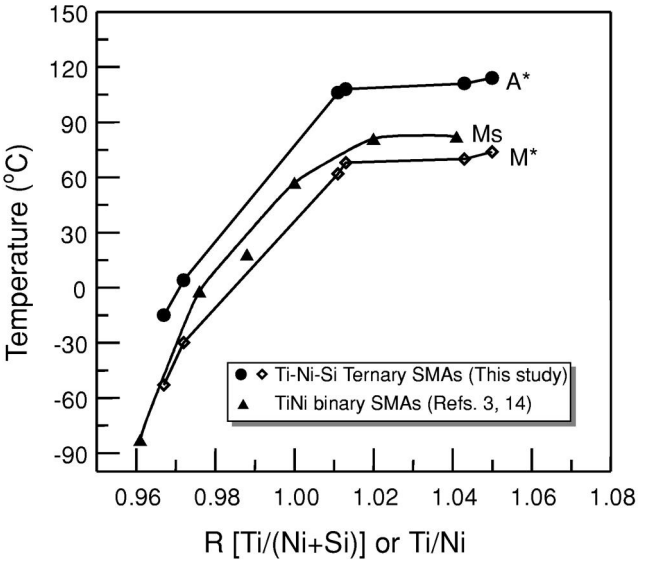

Fig. 3. Transformation temperatures of A* and M* versus *R* ratio for $Ti_{50-x}Ni_{50}Si_x$, $Ti_{50}Ni_{50-x}Si_x$ and $Ti_{51}Ni_{49-x}Si_x$ alloys. The Ms temperature versus Ti/Ni ratio for TiNi binary alloys is also indicated.

of Ti/Ni ratio on the transformation temperature of TiNi binary SMAs is similar to the effect of R ratio on that of $Ti_{49}Ni_{50}Si_1$ and $Ti_{48}Ni_{50}Si_2$ SMAs. The same transformation characteristics can also be found in $Ti_{50}Ni_{49}Si_1$, $Ti_{50}Ni_{48}Si_2$, $Ti_{51}Ni_{48}Si_1$ and $Ti_{51}Ni_{47}Si_2$ alloys. For example, the R ratio of the matrix in $Ti_{51}Ni_{47}Si_2$ alloy is about 1.05, as shown in Table 1, which is nearly equal to the ratio Ti/Ni of $Ti_{51}Ni_{49}$ alloy. The peak temperatures A* and M* of $Ti_{51}Ni_{47}Si_2$ alloy shown in Fig. 2 are nearly equal to those of as-quenched $Ti_{51}Ni_{49}$ alloy [13]. The above fact suggests that the small amount of Si in solid solution in $Ti_{50-x}Ni_{50}Si_x$, $Ti_{50}Ni_{50-x}Si_x$ and $Ti_{51}Ni_{49-x}Si_x$ alloys has an equivalent effect in increasing Ni in TiNi binary alloys. In other words, the substituted Si atoms play a role similar to Ni atoms rather than Ti atoms in TiNi binary alloys. This characteristic is further confirmed by the remarkable consistency in the curves of Fig. 3 in which Ti/Ni ratio is used in as-quenched TiNi binary alloys, but Ti/(Ni+Si) ratio is used in TiNiSi ternary alloys.

Table 2
DSC data of M*, A* and Ms transformation temperatures of $Ti_{50-x}Ni_{50}Si_x$, $T_{50}Ni_{50-x}Si_x$ and $Ti_{51}Ni_{49-x}Si_x$ alloys with $x=1$, 2 at.%

Alloys	M* (°C)	Ms (°C)	A* (°C)
$Ti_{49}Ni_{50}Si_1$	−30	−24	4
$Ti_{48}Ni_{50}Si_2$	−53	−47	−15
$Ti_{50}Ni_{49}Si_1$	61	73	106
$Ti_{50}Ni_{48}Si_2$	68	76	108
$Ti_{51}Ni_{48}Si_1$	70	79	111
$Ti_{51}Ni_{47}Si_2$	74	84	114

4. Conclusion

The TiNi matrix can dissolve a small amount of Si in solid solution, along with three different second phases which were observed in homogenized $Ti_{50-x}Ni_{50}Si_x$, $Ti_{50}Ni_{50-x}Si_x$ and $Ti_{51}Ni_{49-x}Si_x$ alloys with $x=1$, 2 at.%. These are χ-phase particles ($Ti_5Ni_4Si_1$), λ_1-phase particles ($Ti_2Ni_3Si_1$) and Ti_2(Ni, Si) particles. DSC results show that the transformation temperatures for homogenized $Ti_{50-x}Ni_{50}Si_x$, $Ti_{50}Ni_{50-x}Si_x$ and $Ti_{51}Ni_{49-x}Si_x$ alloys with $x=1$, 2 at.% increase with the increasing R ratio (R=Ti/(Ni+Si)) of the matrix. We suggest that the Ni+Si effects on transformation temperatures of Ti–Ni–Si ternary alloys are similar to Ni effects on those of as-quenched TiNi binary alloys. According to this point of view, $Ti_{51}Ni_{49-x}Si_x$ alloys with $x=1$, 2 at.% are similar to Ti-rich TiNi SMAs. They have Ti_2(Ni, Si) second phases when $x=1$ at.% and have Ti_2(Ni, Si) and χ-phase particles when $x=2$ at.%. At the same time, $Ti_{50-x}Ni_{50}Si_x$ and $Ti_{50}Ni_{50-x}Si_x$ alloys with $x=1$, 2 at.% can be regarded as Ni-rich or near equiatomic TiNi SMAs. They only have χ-phase particles as the second phase when $x=1$ at.%, and have χ-phase and λ_1-phase particles when $x=2$ at.%. Experimental results also show that $Ti_{50}Ni_{48}Si_2$ alloy

which behaved similarly to $Ti_{50}Ni_{50}$ SMA has the greatest amount of Si in solid solution in the matrix.

Acknowledgements

The authors are pleased to acknowledge the financial support provided for this research by the National Science Council (NSC), Republic of China under Grant NSC 89-2216-E151-010 and NSC 88-2216-E002-013.

References

[1] S. Miyazaki, Y. Igo, K. Otsuka, Acta Metall. 34 (1986) 2045.
[2] S.K. Wu, H.C. Lin, T.S. Chou, Script. Metall. 23 (1989) 2043.
[3] M. Nishida, T. Honma, Script. Metall. 18 (1984) 1293.
[4] H.C. Lin, S.K. Wu, T.S. Chou, H.P. Kao, Acta Metall. 39 (1991) 2069.
[5] K.H. Eckelmeyer, Script. Metall. 10 (1976) 667.
[6] T. Honma, M. Matsumoto, Y. Shugo, M. Nishida, I. Yamazaki, in: H. Kimura, O. Izumi (Eds.), Proceedings 4th International Conference on Titanium '80, AIME, Warrendale, PA, 1980, p. 1455.
[7] C.M. Hwang, M. Meichle, M.B. Salamon, C.M. Wayman, Phil. Mag. 47A (1983) 177.
[8] S.K. Wu, C.M. Wayman, Metallography 20 (1987) 359.
[9] Y.C. Lo, S.K. Wu, C.M. Wayman, Script. Metall. 24 (1990) 1571.
[10] P.G. Lindqist, C.M. Wayman, in: T.W. Duering, K.N. Melton, D. Stockel, C.M. Wayman (Eds.), Engineering Aspects of Shape Memory Alloys, Butterworth Heinemann, London, 1990, p. 58.
[11] Y. Nakata, T. Tadaki, K. Shimizu, Mater. Trans., JIM 32 (1991) 1120.
[12] T. Nam, T. Saburi, Y. Kawamura, K. Shimizu, Mater. Trans., JIM 31 (1990) 262.
[13] M. Nishida, C.M. Wayman, T. Honma, Metall. Trans. 17A (1986) 1505.
[14] H.C. Lin, S.K. Wu, J.C. Lin, Mater. Chem. Phys. 37 (1994) 184.
[15] P. Villars, A. Prince, H. Okamoto, in: Handbook of Ternary Alloy Phase Diagrams, Vol. 10, ASM International, Pittsburgh, USA, 1995, p. 13026.
[16] S.F. Hsieh, S.K. Wu, H.C. Lin, J. Alloys Comp. (2001) in press.